

Alignment of ADS beta cryostat with wire position monitor*

ZHU Hong-Yan (朱洪岩),[†] DONG Lan (董岚), MEN Ling-Ling (门瓴玲), LIU Can (刘璨), and LI Bo (李波)

Institute of High Energy Physics, Chinese Academy of Sciences, Beijing 100049, China

(Received August 25, 2014; accepted in revised form October 10, 2014; published online August 20, 2015)

Wire position monitor (WPM) is designed to monitor contraction of the cold masses during the cooling-down operation in an accelerator driven system. Because of material difference, machining error, assembly error, etc., each WPM has to be calibrated. The sensing voltage and wire position are of a nonlinear relationship, which is expressed by high order polynomial. Root mean square (RMS) of the polynomial fitting error were $3.8\ \mu\text{m}$ and $7.4\ \mu\text{m}$ at x and y directions, respectively. The alignment test was carried out on the beta cryostat. Optical instruments were used to verify the WPM measuring results. The differences between WPM measuring results and optical measurements were 0.044 and 0.05 mm in x and y direction, respectively. A significant asymmetric contraction was detected, and asymmetry of material was taken as the main reason through analysis.

Keywords: Wire position monitor, Alignment of cryostat, Wire position monitor calibration

DOI: 10.13538/j.1001-8042/nst.26.040401

I. INTRODUCTION

An accelerator driven system (ADS) is being developed at IHEP (Institute of High Energy Physics, Chinese Academy of Sciences). Most cavities and magnets are working in the cryostat at liquid Helium (LHe) temperature. Each cryostat has 6 superconducting cavities and 5 superconducting magnets. Their alignment will be carried out at room temperature first, and after contraction the positional error of the cavities and magnets shall be within ± 0.1 mm [1, 2]. The conventional collimation methods are difficult to be implemented to measure the targets within the cryostat, and the material contraction shall be monitored during the thermal cycle, so a wire position monitor (WPM) was designed to monitor the position change caused by contraction and expansion [3–5]. The design and machining of WPM has already completed [6].

Because of the material difference, machining error, assembly error, etc., each WPM has to be calibrated before using. A platform was designed to calibrate the WPMs. Then alignment experiment was carried out on the beta cryostat. Optical instruments were used to verify the WPM measurement results.

II. SIMULATION

A. Calibration simulation

The calibration simulation results [7], on CST microwave studio within ± 4 mm in 0.5 mm steps, are shown in Fig. 1.

K_x and K_y , functions of the wire position x and y , are defined as

$$K_x = x/U, \quad K_y = y/V, \quad (1)$$

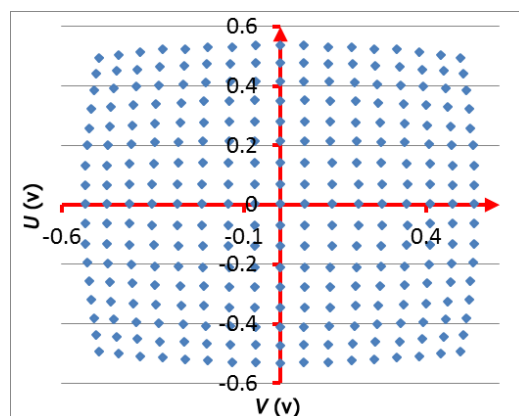


Fig. 1. (Color online) The U - V map (in voltage) obtained by calibration simulation.

where U and V are the sensing voltage in wire position x and y , respectively. K_x and K_y are approximately constant when x and y are small. Because of the probe geometry of and the microstrip angle, the relationship between the sensing voltage and wire position in each direction is not linear. High order polynomial can be used to express the relationship [1, 8]

$$x = \sum_{i=0}^k \sum_{j=0}^{k-i} A_{ij} U^i V^j, \quad y = \sum_{i=0}^k \sum_{j=0}^{k-i} B_{ij} U^i V^j, \quad (2)$$

where A and B are polynomial coefficients of each direction, and k is the order of polynomial, which can adjusted according to the calibration result.

B. Influence of WPM's position error

The inner radius of WPM is 12 mm. The microchips were 1 mm wide and 76 mm long, and their height is calculated to achieve the $50\ \Omega$ match with the reading out circuits [1]. The wire position monitor is supported by a low expansion coefficient insulation material G10 in cryostat. The set-up is

* Supported by the Project of Injector I Mechanical & Technical Support System

[†] Corresponding author, zhuhy@ihep.ac.cn

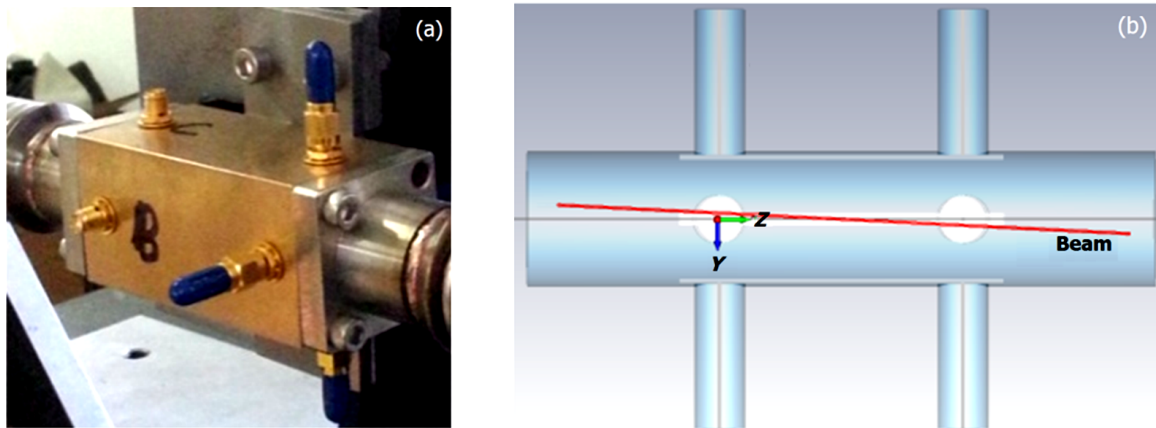


Fig. 2. (Color online) The WPM on the platform (a) and the simulation sketch (b).

placed on a steel platform. The connection structure between platform and WPM is shown in Fig. 2(a). Due to the assemble error, the WPM may not be parallel with the wire. Four sets of simulations were done to analyze the influence of this position error. The coordination system is aligned with the center of WPM and the end of the microstrip (Fig. 2(b)). Simulated position errors caused by wire tilting in 0.5° steps are given in Table 1, where L is the length of the strip and the coordinates are rotate centers in each simulation.

TABLE 1. Position errors caused by wire tilt

Tilt angle (degree)	$x = 0, y = 0, z = L/2$	$x = 0, y = 0, z = L/4$	$x = 0, y = 0, z = 0$	$x = 0, y = 2, z = L/2$
0	0.000	0.000	0.000	0.017
0.5	0.002	-0.068	-0.145	0.110
1.0	0.020	-0.165	-0.318	0.273
1.5	0.038	-0.204	-0.403	0.415
2.0	0.047	-0.235	-0.572	0.584
2.5	0.059	-0.315	-0.656	0.733
3.0	0.068	-0.342	-0.782	0.908

The readout sensing signal is a superposition of upstream signal and reflection of downstream signal [6]. Amplitudes of the two signals should be the same. The readout signal actually reflects the center position of the wire. So, a position calculated by a calibration simulation result is compared with the real center position of the wire, and each value in Table 1 is the error between them. From Table 1, one sees that the further the tilt center from the WPM center, the bigger the error is. If the tilt center is at the WPM center, the error can be ignored within $\pm 2^\circ$. But the error cannot be ignored even within 0.5° when tilt center changes.

Electronic level, optical level and theodolite were used to adjust the relative position between the WPM probe and the wire. The electronic level was used to level WPM probe. The optical level was used to level the wire. The theodolite was used to adjust parallelism of the vertical lines in the horizontal plane, which can be guaranteed within $10''$.

III. CALIBRATION PLATFORM

The WPM contains four Cu antennas supported by SMA jacks. The upstream ports are connected to the readout electronics to measure the signal amplitude, while the downstream ports are terminated by a $50\ \Omega$ loads. The monitor body is made of Cu, too.

A. Platform structure

In the calibration platform (Fig. 3), a fixed stretch wire acts as a reference [9, 10] and signal carrier fed by 215 MHz RF signal [5, 11, 12]. The WPM is attached to an electric translator stage with a high position resolution up to $2\ \mu\text{m}$. The platform takes the WPM to move around to simulate material contraction. The sensing signal of four microstrip-antennas changes with the movement, and the signal amplitude can correspond to a certain displacement after calibration [13, 14].

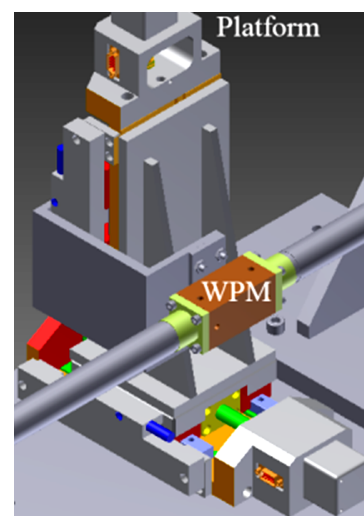


Fig. 3. (Color online) Calibration stand with WPM, translator stage and bellows.

B. Input and termination structure

The wire connection with external RF signal and the matching load are made in the two external boxes (Fig. 4). The input side is fixed, and the other side is loaded with a set of steel blocks. At both sides, the copper beryllium wires are allowed to slide on the G10 pulley during contraction or expansion. The wire edges are clamped between G10 blocks, the total weight of steel blocks are 5 kg [15].

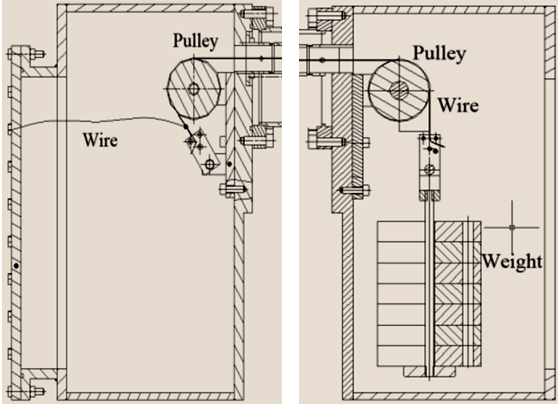


Fig. 4. (Color online) The RF input and termination.

C. Data acquisition

Figure 5(a) is a diagram of the data processing circuits. A time-sharing system is used. The digital IO controls RF switches for the WPMs [16]. The signals from the monitor are processed by a bergoz card, and transferred to a PC through DAQ card to calculate wire position by coefficients calibrated. The sensing signals are shown in Fig. 5(b).

IV. WPM CALIBRATION

The SMA jacks use PTFE insulation, which contracts as temperature goes down. This common mode contraction in symmetric structure will be cancelled in differential circuits. Experiment results show that the reading difference between LN_2 and room temperature is about 0.04 mm, which is partially caused by body contraction or temperature differential. So, the wire position monitor is only calibrated at room temperature. We did two calibration tests, one is within $r/2$ (± 6 mm) in step of 0.2 mm, the other is within $r/3$ (± 4 mm) in step of 0.1 mm (Fig. 6). $U-V$ is the sensing voltage at each position. 100 mV corresponds to 0.1 mm displacement at the center.

We use sixth-order polynomial in $r/2$ (± 6 mm) mapping and fourth-order in $r/3$ (± 4 mm) mapping. The fitting results of $r/3$ (± 4 mm) mapping are given in Table 2.

The coefficients A_{00} and B_{00} at U^0V^0 are offset between the geometry center and electrical center of each direction.

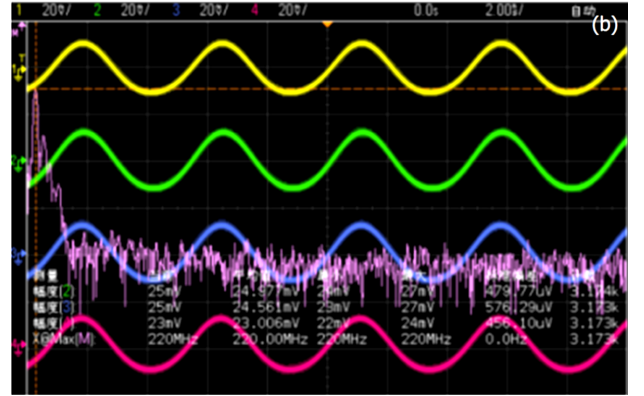
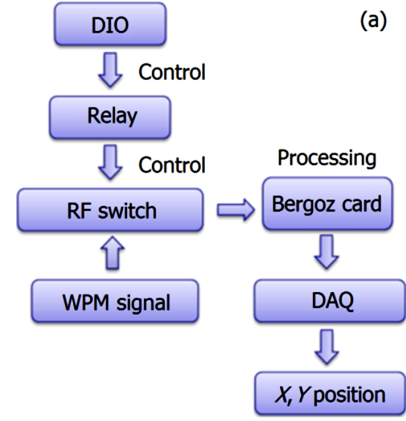


Fig. 5. (Color online) Block diagram of the data acquisition electronics (a) and signals at the four pickups (b).

TABLE 2. The calibration coefficient (in mm) of ± 4 mm

	A_{ij}	B_{ij}
U^0V^0	-7.21×10^{-3}	-2.83×10^{-3}
U^0V^1	1.71×10^{-6}	-1.51×10^{-3}
U^0V^2	8.42×10^{-10}	2.22×10^{-10}
U^0V^3	1.60×10^{-13}	-3.93×10^{-11}
U^0V^4	1.58×10^{-16}	-1.11×10^{-16}
U^1V^0	-1.51×10^{-3}	-6.67×10^{-7}
U^1V^1	-2.21×10^{-10}	7.74×10^{-9}
U^1V^2	-3.79×10^{-11}	1.51×10^{-13}
U^1V^3	-8.58×10^{-18}	-2.00×10^{-16}
U^2V^0	-8.28×10^{-9}	-2.75×10^{-11}
U^2V^1	1.11×10^{-13}	-3.42×10^{-11}
U^2V^2	-1.33×10^{-16}	6.01×10^{-17}
U^3V^0	-3.20×10^{-11}	7.00×10^{-15}
U^3V^1	1.51×10^{-17}	9.24×10^{-16}
U^4V^0	1.33×10^{-15}	-9.51×10^{-17}

The offset is $-7.2 \mu\text{m}$ at x direction, and $-2.8 \mu\text{m}$ at y direction. A_{01} and B_{10} are the first order coefficients which represent position resolution, the smaller the better. The fitting results in ± 4 mm and ± 6 mm are consistent. The variances of fitting error are as following [8]

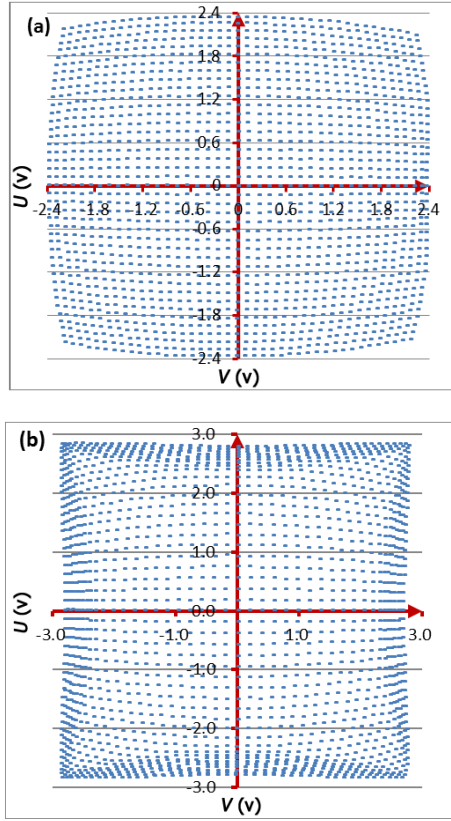


Fig. 6. (Color online) U - V mapping within $r/3$ (± 4 mm) in 0.1 mm steps (a) and $r/2$ (± 6 mm) in 0.2 mm steps (b).

$$\begin{aligned}
 S_{x-4\text{ mm}} &= \sqrt{\frac{\sum_{p=1}^n (x_{0p} - x_p)^2}{n}} = 3.8 \mu\text{m}, \\
 S_{y-4\text{ mm}} &= \sqrt{\frac{\sum_{p=1}^n (y_{0p} - y_p)^2}{n}} = 7.4 \mu\text{m}, \\
 S_{x-6\text{ mm}} &= 0.047 \text{ mm}, \quad S_{y-6\text{ mm}} = 0.045 \text{ mm}.
 \end{aligned}
 \tag{3}$$

As shown in Fig. 7, the fitting error of ± 6 mm is much bigger than that of ± 4 mm.

V. ALIGNMENT EXPERIMENT

A. Experiment setup

A complete thermal cycle was carried out on the beta-cryostat designed for alignment test only. The beta-cryostat was 2 m long. There were four WPMs symmetrically assembled beside the $\Phi 1$ m cavity made of 316 steel, the same material with its girder. A schematic layout of the WPMs and optical targets is shown in Fig. 8. The parts in blue is made of G10 material. Having low thermal conductivity and low thermal deformation [5], it is used as support of the WPMs and optical targets and the bottom insulation layer.

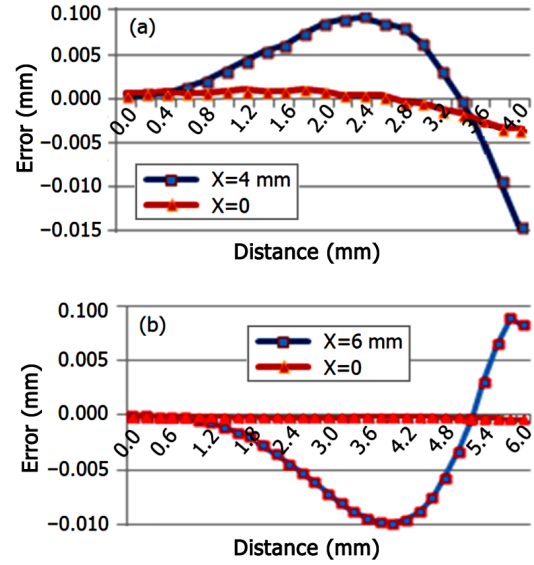


Fig. 7. (Color online) Fitting error of ± 4 mm (a) and ± 6 mm (b), as a function of distance from the center.

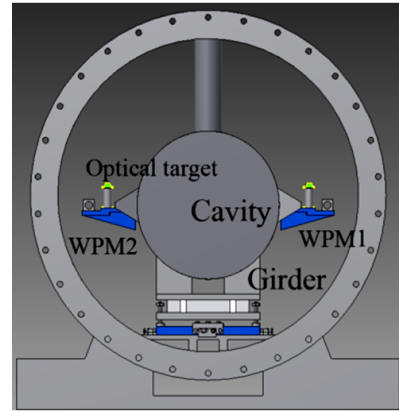


Fig. 8. (Color online) Schematic layout of WPMs and optical targets.

When the temperature drops down, the cavity and its girder will contract. Attached to the cavity, a WPM will suffer a displacement at both horizontal and vertical directions [17, 18]. The contraction of major concern happens between the cavity center and the girder bottom. The distance between them was 0.419 m. The two optical targets placed at one end of the cryostat on the same support with WPM had the same displacement with WPM. Levels was used to measure vertical displacement of the optical targets, and theodolites to measure the horizontal displacement. The optical measurements and the WPM measurements were compared to check the correctness.

B. Experiment procedure

The beta-cryostat evacuation started at 8:00 on June 10, 2014, and the vacuum reached 0.1 Pa about 3 h later. Figure 9

shows horizontal and vertical displacements of the beta-cryostat during the whole thermal cycle.

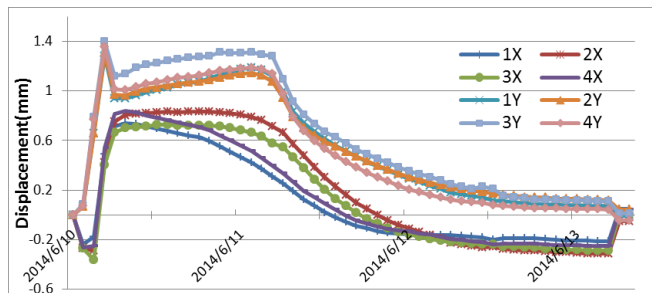


Fig. 9. (Color online) Historical graph of horizontal and vertical displacement of beta-cryostat cold mass during the whole thermal cycle.

At the beginning, a positive movement can be seen in both vertical and horizontal direction, as an effect of evacuation. The cool-down procedure started right after the vacuum reached 0.1 Pa. Liquid N_2 was pumped into the $\Phi 1$ m cavity, which suffered a sharp change in displacement. After a little recovery from the sudden change, the contraction increased as the temperature went down [19]. From the figures, we can see the contractions were not symmetrical, especially in the x direction. The maximum contraction difference in x direction was 0.4 mm, and the maximum difference in y direction was 0.2 mm. This asymmetric contraction may cause a shift of the facility center. So, guaranteeing the girder material's symmetry should be of a major consideration [20, 21].

The warm-up started at 12:00 on June 11. This procedure was much slower than cool-down. The position is well recovered from the vertical and horizontal displacement after

warm up. The optical measurement was slow, so all the measurements were taken at the stable change period. Figure 10 shows the error between optical and WPM measurements. The difference between WPM and optical measurements are within 0.1 mm. The variance of the difference is 0.044 mm in x direction and 0.05 mm in y direction. Considering the alignment error and the self-contraction of optical target, the measurement results are consistent.

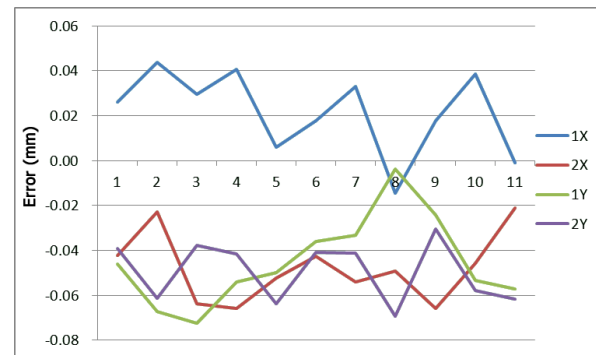


Fig. 10. (Color online) Error between optical and WPM measurement.

VI. CONCLUSION

The comparison results between optical measurements and WPM measurements show that the measurement of WPM is credible. The use of optical instrument involves personnel and the readings can be taken only periodically. Conversely, the WPM can monitor continuously providing detailed contraction data which is valuable to help characterize new structures.

- [1] Bosotti A, Pagani C and Varisco G. Online monitoring of the TTF cryostats cold mass with wire position monitors. INFN-LNF-TC-00-2, 2000.
- [2] Bedeschi F, Bellettini G, Bosotti A, *et al.* A new wire position monitor readout system for ILC cryomodules. IEEE Nucl Sci Conf R, 2007, 1684–1686. DOI: [10.1109/NSS-MIC.2007.4437324](https://doi.org/10.1109/NSS-MIC.2007.4437324)
- [3] Eddy N, Fellenz B, Prieto P, *et al.* A wire position monitor system for the 1.3 GHz tesla-style cryomodule at the fermilab New-Muon-Lab accelerator. 15th International Conference on RF Superconductivity(SRF2011), Chicago, Illinois, USA, Jul. 25–29, 2011. arxiv: [1209.4917](https://arxiv.org/abs/1209.4917)
- [4] Zhang D. A wire position monitor for superconducting cryomodules at fermilab. BIW'10, Santa Fe, NM, USA, May 2010, 187–188.
- [5] Rawnsley W R, Giove D. ISAC-II cryomodule alignment monitor, TRIUMF Design Note, TRI-DN-03-02, 2003.
- [6] Zhu H Y, Dong L and Li B. Design and simulation of a wire position monitor for cryogenic systems in an ADS linac. Chinese Phys C, 2014, **38**: 087001. DOI: [10.1088/1674-1137/38/8/087001](https://doi.org/10.1088/1674-1137/38/8/087001)
- [7] He X Y and Wu J. Calibration method of HLS's sensor used in SSRF. Nucl Sci Tech, 2008, **19**: 321–324. DOI: [10.1016/S1001-8042\(09\)60011-7](https://doi.org/10.1016/S1001-8042(09)60011-7)
- [8] Ruan Y F. The study of the beam instruments for CSNS LINAC. Ph.D. Thesis, China Academy of Sciences, 2010. (in Chinese)
- [9] Bowden G. Stretched wire mechanics. IWAA, TS08-3, CERN, Geneva, Switzerland, Oct. 2004.
- [10] Wei M. Research on microstructure and mechanical properties of glass fiber/polyuria composites. Ph.D. Thesis, Harbin Institute of Technology, 2013. (in Chinese)
- [11] Rawnsley W R. Alignment of the ISAC-II medium beta cryomodule with a wire monitoring system. 20th International Cryogenic Engineering Conference, Beijing, China, 2004.
- [12] Bosotti A, Pagani C, Paparella R, *et al.* Mechanical vibration measurements on TTF cryomodules. IEEE Part Acc Conf, 2005, 434–436. DOI: [10.1109/PAC.2005.1590460](https://doi.org/10.1109/PAC.2005.1590460)
- [13] Bosotti A. The wire position monitor(WPM) as a sensor for mechanical vibration for the TTF cryomodules. SRF'05, Cornell University, Ithaca, New York, USA, July 2005, 558–562.
- [14] Stanford G, Bylinsky Y and Laxdal R E. Engineering and cryogenic testing of the ISAC-II medium beta cryomodule. Pro-

- ceedings of LINAC 2004, Lübeck, Germany, 2004, 630–632.
- [15] Deibele C. Matching BPM stripline electrodes to cables and electronics. Proceedings of 2005 Particle Accelerator Conference, Knoxville, Tennessee, 2005, 2607–2609.
- [16] PCI1734 Digital IO Users' manual. Adcantech, Beijing, 2008.
- [17] Shafer R E. Beam position monitor sensitivity for low-beta beams. AIP Conf Proc, **319**: 303–308. DOI: [10.1063/1.46975](https://doi.org/10.1063/1.46975)
- [18] Giove D, Bosotti A, Pagani C, *et al.* A wire position monitor (WPM) system to control the cold mass movements inside the TRF cryomodule. IEEE Part Acc Conf, 1997, **3**: 3657–3659. DOI: [10.1109/PAC.1997.753375](https://doi.org/10.1109/PAC.1997.753375)
- [19] Forck P, Kowina P and Liakin D. Beam position monitor. Helmholtz Centre for Heavy Ion Research GSI. Germany, 2008.
- [20] Suwada T, Kamikubota N, Fukuma H, *et al.* Stripline-type beam-position-monitor system for single-bunch electron/positron beams. Nucl Instrum Meth A, 2000, **440**: 307–319. DOI: [10.1016/S0168-9002\(99\)00960-2](https://doi.org/10.1016/S0168-9002(99)00960-2)
- [21] Shintake T, Tejima M, Ishii H, *et al.* Sensitivity calculation of beam position monitor using boundary element method. Nucl Instrum Meth A, 1987, **254**: 146–150. DOI: [10.1016/0168-9002\(87\)90496-7](https://doi.org/10.1016/0168-9002(87)90496-7)